NONLINEAR SIMULATIONS OF SURFACE WAVES IN FINITE DEPTH ON A LINEAR SHEAR CURRENT

Marc Francius[1], Christian Kharif[2], Sylvain Viroulet[3]

Abstract

This study concerns the propagation of surface gravity waves on a linear shear current over a constant water depth. It is restricted to two-dimensional flows without dissipation and/or wind effects. Numerical simulations of nonlinear surface waves on a linear shear current (constant vorticity) are performed using an extension of the well-known high-order spectral method (HOS). An adjustment procedure for initializing the nonlinear free surface simulations with linear solutions is validated, and used to study the nonlinear stability of a uniform wave train in finite depth. It is shown that small positive velocity shear tends to enhance the sideband instabilities, whereas small negative velocity shear tends to suppress instability.

Key words: Surface gravity waves, finite depth, linear shear current, modulational instability, HOS method.

1. Introduction

In many coastal applications the currents, corresponding to a background mean flow, cannot be neglected and may have an important influence on surface waves dynamics. Owing to previous studies of the wave-current interactions, which are well documented in the review articles by Peregrine (1976), Jonsson (1990) and Thomas and Klopman (1997), the study of surface waves dynamics on a vertically varying current has attracted much less attention than that on a horizontally varying current. In the latter case, where the background flow is allowed to vary slowly in the horizontal directions, much attention has been given to the effects of the large amplitudes of waves on the corresponding slow modulations of the wave amplitudes and wavenumbers. Modern theories on this problem were initiated by Longuet-Higgins and Stewart (1961), Whitham (1965)and Bretherton and Garrett (1968), in which the concept of radiation stress was introduced and the action conservation equation was established for the case of irrotational current. On the other hand, if there is current variation with depth the flow is usually strongly rotational, and a theoretical description of unsteady surface waves in such flows is non-trivial, in particular, when nonlinear effects become important.

In the last few years, there has been a growing interest in nonlinear periodic water waves in finite depth on arbitrary shear flows. Surface water waves propagating steadily on a rotational current have been studied by many authors. Among them, one can cite Tsao (1959), Dalrymple (1974), Brevik (1979), Simmen and Safmann (1985), Teles da Silva and Peregrine (1988), Kishida and Sobey (1988), Ko and Strauss (2008), Pak and Chow (2009), Constantin (2011), etc. We note that, although the recent important theoretical developments have confirmed that periodic waves can exist over flows with arbitrary vorticity, their stability and their nonlinear evolution have not been much studied extensively so far. In fact, even in the rather simple case of uniform vorticity (linear shear), few papers have been published on the effect of a vertical shear current on the side-band instability of a uniform wave train over finite depth. It is noted here that this instability is often referred in the literature as the Benjamin-Feir or modulational instability.

Johnson (1976) studied the slow modulation of a harmonic wave on a two dimensional flow of arbitrary

[1]Université de Toulon, CNRS/INSU, IRD, MOI, UM 110, 83957 La Garde, France. francius@univ-tln.fr
[2]IRPHE, UMR 6594 , 49 rue F. Joliot Curie BP 146, Marseille 13384, France. kharif@irphe.univ-mrs.fr
[3]IRPHE, UMR 6594 , 49 rue F. Joliot Curie BP 146, Marseille 13384, France. viroulet@irphe.univ-mrs.fr

vorticity. Using the method of multiple scales he obtained the condition of linear stability for a nonlinear plane wave or uniform wave train. This condition is verified if the product of the dispersive and nonlinear terms of the nonlinear Schrödinger equation (NLS equation) is negative. Using the same approach, the stability properties of weakly nonlinear wave packets to three dimensional perturbations have been studied by Oikawa et al. (1987). Their analysis was illustrated for the case of a linear shear. In both studies, unfortunately, the resulting third-order envelope equations possess coefficients that depend in a complicated way on the shear, and are thus not practical to use. To avoid this, Thomas et al. (2012) derived a vor-NLS equation in finite depth when the vorticity is taken into account, using also the method of multiple scales but with different scalings. The resulting coefficients of the vor-NLS equation are given explicitly as a function of the vorticity and depth of shear layer. These authors also carried out a stability analysis of a weakly nonlinear wave train in the presence of uniform vorticity. They demonstrated that vorticity modifies significantly the modulational instability properties of weakly nonlinear plane waves, namely the growth rate and bandwidth of the unstable side-band modes. They also showed that these plane wave solutions may be linearly stable to modulational instability independently of the dimensionless depth kh.

In addition, there has been a renewed interest in numerical simulations of this problem using the exact nonlinear equations. Okamura and Oikawa (1989) investigated numerically the linear stability of two-dimensional finite amplitude surface waves on a linear shear flow to three-dimensional infinitesimal rotational disturbances. Concerning the nonlinear stability and evolution of uniform wave train, results were presented only for the deep water case. Nwogu (2009) reported results about the modulational instability of gravity waves on an exponentially sheared current. His numerical results demonstrated that the mean flow vorticity can significantly affect the growth rate of extreme waves in narrow band sea states. Choi (2009) considered the Benjamin-Feir instability of a modulated wave train in both positive and negative shear currents within the framework of the fully nonlinear water wave equations. For fixed wave steepness, he compared his results with the irrotational case and found that the envelope of the modulated wave train grows faster in a positive shear current and slower in a negative one.

In this paper we use an adaptation of the well-known high-order spectral method (HOS) to calculate the nonlinear time evolution of small amplitude modulations on two-dimensional wave trains in finite depth and in the presence of a linear shear current. The reason for the choice of background flow is twofold. First many significant currents, for example, induced by coastal tides or encountered in rivers, are well-modelled by constant vorticity. Secondly, for a background flow with constant vorticity, the wave motions can be treated as irrotationnal motions (if initially they are so), and the approach to derive the system of nonlinear evolution equations for irrotational waves in finite depth can be readily applied to the case with a linear shear current.

2. Mathematical formulation

Consider an incompressible flow of an inviscid, homogeneous fluid bounded by a free surface near $z=0$ and a flat bottom boundary at $z=-h$. The equations of motion then are the Euler equations

$$\partial_t u + u\partial_x u + v\partial_y u + w\partial_z u = -\frac{1}{\rho}\partial_x p \tag{1}$$

$$\partial_t v + u\partial_x v + v\partial_y v + w\partial_z v = -\frac{1}{\rho}\partial_y p \tag{2}$$

$$\partial_t w + u\partial_x w + v\partial_y w + w\partial_z w = -\frac{1}{\rho}\partial_z p - g \tag{3}$$

and the incompressibility condition,

$$\partial_x u + \partial_y v + \partial_z w = 0 \tag{4}$$

where g is the gravitational acceleration, p the total pressure and (u,v,w) the components of the total velocity vector. The fluid has also to satisfy the usual kinematic and dynamic boundary conditions at the free surface,

$$\partial_t \zeta = w - u\partial_x \zeta - v\partial_y \zeta \quad \text{at} \quad z = \zeta \tag{5}$$

$$p = p_{atm} \quad \text{at} \quad z = \zeta \tag{6}$$

and a kinematic boundary condition at the bottom,

$$w = 0 \quad \text{at} \quad z = -h \tag{7}$$

Although this system of equations admits an exact solution, given by any steady current flowing below a flat surface, exact solutions are in general unknown when a surface wave is present. For a general rotational combined wave-current field, the total velocity field consists of 2 components: a mean component, (U(z),V(z),0) which corresponds to a steady vertically sheared current field, and a component associated with the orbital wave motions.

2.1. ***Fully nonlinear two-dimensional equations***

Since the choice of the directions of the x and y axes is arbitrary, it is convenient to choose the y axis parallel to the wave crests so that all variables are independent of y for two-dimensional free surface flows. To simplify furthermore, we assume that the current is in one direction only, the x-axis chosen in the direction of wave propagation and thus v=V= 0.

Not only the two dimensional configuration can provide a good approximation in many practical cases, but it also allows to simplify the description of the fluid motion by introducing a stream function $\Psi(x,z,t)$, defined up to a constant as $u = \partial\Psi / \partial z$ and $u = -\partial\Psi / \partial x$. By definition of the vorticity, we have

$$\nabla^2 \Psi = -\Omega_0 \tag{8}$$

which shows that $\Psi(x,z,t)$ is solution of a Poisson equation, together with the constant pressure dynamic boundary condition (Eq. 6) and kinematic boundary conditions (Eqs. 5 and 7). More importantly, with a linear shear current defined by a surface velocity U_0 and vorticity Ω_0 (constant), namely $U(z)=U_0+\Omega_0 z$, the equation for wave-induced vortiticy decouples from the mean flow. Consequently, two dimensional wave perturbations must remain irrotational if initially they are so. Hence the approach to derive the system of nonlinear evolution equations for irrotational waves can be readily applied to the case considered here, i.e. two dimensional irrotational perturbations propagating on a linear shear current.

For this type of wave motions $\Psi(x,z,t)$ can be rewritten as the sum of a particular integral satisfying Eq. 8 and an irrotational stream function $\psi(x,z,t)$ associated with the wave perturbations. By writting, for instance,

$$\Psi(x,z,t) = \psi(x,z,t) + \frac{1}{2}\Omega_0 z^2 + U_0 z \tag{9}$$

we find that ψ is a harmonic function and therefore has a (harmonic) conjugate function $\phi(x,z,t)$ such that $\partial\psi/\partial z = \partial\phi/\partial x$ and $\partial\psi/\partial x = -\partial\phi/\partial z$. The stream function and the (generalized) velocity potential ϕ, describe the same irrotational perturbation of the linear shear current, and ϕ also satisfies the Laplace's equation within the fluid.

Then, in terms of the functions ϕ and ψ, we can recast the Euler equations in the form of a generalized Bernouilli equation for two-dimensional irrotationnal waves and a linear shear current. This yields the following relation for the pressure field within the fluid,

$$-\frac{p}{\rho} = \partial_t\phi + gz + \frac{1}{2}\left[\left(\partial_x\phi\right)^2 + \left(\partial_z\phi\right)^2\right] + \left(U_0 + \Omega_0 z\right)\partial_x\phi - \Omega_0\psi + \frac{1}{2}U_0^2 \tag{10}$$

and the dynamic boundary condition at the free surface can then be written as,

$$\partial_t\phi + g\zeta + \frac{1}{2}\left[\left(\partial_x\phi\right)^2 + \left(\partial_z\phi\right)^2\right] + \left(U_0 + \Omega_0\zeta\right)\partial_x\phi - \Omega_0\psi_s = 0 \tag{11}$$

where $\psi_s = \psi(x,\zeta,t)$ is the irrotational stream function evaluated at the free surface. Without loss of generality, we have absorbed $U_0^2/2$ in the definition of ϕ and choose $p_{atm} = 0$.

In order to further simplify and reduce the dimension of the water wave problem, it is convenient to introduce $\phi_s = \phi(x,\zeta,t)$, the velocity potential evaluated at the free surface, and to use the relations

$$\partial_t\phi_s = \partial_t\phi\big|_{z=\zeta} + \partial_t\zeta\cdot W, \qquad \partial_x\phi_s = \partial_x\phi\big|_{z=\zeta} + \partial_x\zeta\cdot W \tag{12}$$

where $W(x,t)$ is the surface vertical component of the velocity. With these dependent surface fields, it is then possible to derive a couple of exact evolution equations

$$\partial_t\zeta = \left(1+\left(\partial_x\zeta\right)^2\right)W - \partial_x\zeta\cdot\partial_x\phi_s - \left(U_0 + \Omega_0\zeta\right)\cdot\partial_x\zeta \tag{13}$$

$$\partial_t\phi_s = -g\zeta - 0.5\left(\partial_x\zeta\right)^2 + 0.5\left[1+\left(\partial_x\zeta\right)^2\right]W^2 - \left(U_0 + \Omega_0\zeta\right)\cdot\partial_x\phi_s + \Omega_0\psi_s \tag{14}$$

where W is the vertical component of the surface velocity. The solution to these equations relies on the evaluation of W and ψ_s as a function of the elevation ζ and the surface velocity potential ϕ_s, in which case the system (Eqs. 13- 14) is closed and constitutes a set of nonlinear equations in these two surface field variables. This can be achieved using the following relationship for two dimensional wave motions

$$\partial_x\psi_s = -G(\zeta)\phi_s = -\left[1+\left(\partial_x\zeta\right)^2\right]\hat{G}(\zeta)\phi_s + \partial_x\zeta\cdot\partial_x\phi_s \tag{15}$$

as well as boundary perturbation and Taylor series expansion techniques to compute high-order approximations of the non local operators G and $\hat{G}$. The Dirichlet Neumann operator (DNO) G maps the surface velocity potential ϕ_s to an unnormalized normal velocity evaluated at the surface, while $\hat{G}$ maps ϕ_s to the vertical velocity evaluated at the surface, namely $W = \hat{G}\phi_s$. In practice, for small to moderate amplitude the Taylor series for G and $\hat{G}$ are rapidly convergent, and may be truncated at a relatively low order of truncature *M*.

For irrotational flows without currents, $U_0 = 0$ and $\Omega_0 = 0$, this formulation is commonly referred to as the high-order spectral (HOS) method. The HOS method has been proposed independently by Dommermuth & Yue (1987) and West et al. (1987) for the modelling of nonlinear water waves over constant or infinite depth, and later extended by Liu & Yue (1998) and Smith (1998) to include the effects

of bottom topography.

2.2. *Weakly nonlinear equations*

As already mentioned, very few studies have been proposed to describe the slow modulation of weakly nonlinear wave trains in the presence of arbitrary vorticity. In the majority of cases, asymptotic expansions and multiple scales method have been used to obtain envelope evolution equations, which allow eventually to formulate a condition of stability to long modulational perturbations.

Following Thomas (2012), weakly nonlinear wave trains that are modulated on a slow time scale $\tau = \varepsilon^2 t$ and slow characteristic scale $\xi = \varepsilon\left(x - c_g t\right)$ can be assumed to be written as

$$\zeta = \sum_{n=0}^{\infty} \varepsilon^n \sum_{j=n}^{\infty} \varepsilon^j a_{nj}\left(\xi, \tau\right) E^n + c.c. \tag{16}$$

where ε is a measure of wave amplitude, $E = \exp\left[ik_0\left(x - c_p t\right)\right]$, $c_p = \omega / k_0$ is the linear phase velocity and c_g the group velocity of the leading harmonic carrier wave with wavenumber k_0 and frequency ω. To the leading order in wave amplitude, the wave train can be approximated as

$$\zeta = \frac{1}{2} a \exp\left[ik_0\left(x - c_p t\right)\right] + c.c. \tag{17}$$

where $a = a_{11}\left(\xi, \tau\right)$ is the complex amplitude modulation function. To third order in the wave amplitude, the vor-NLS equation is obtained in the form,

$$ia_\tau + La_{\xi\xi} = M\left|a\right|^2 a \tag{18}$$

after tedious substitutions of the above series expansions in the governing equations, and also appropriate Taylor expansions of the free surface boundary conditions. The details of the procedure and the expression of the coefficients of dispersion *L* and nonlinearity *M* are given explicitly in Thomas (2012).

As is well-known, this vor-NLS equation admits the uniform wave train solution given as $a\left(\xi, \tau\right) = a_0 \exp\left(-iMa_0^2 \tau\right)$, where a_0 is an arbitrary constant and the phase argument represents the well-known second-order correction to the frequency or, equivalently, phase velocity of the carrier wave. As usual, the linear stability problem is examined by writing $a\left(\xi, \tau\right) = a_0\left(1 + \delta_a\right)\exp\left(i\left(\delta_\omega - Ma_0^2 \tau\right)\right)$, which represents a general perturbation of the uniform wave train. After substitution in Eq. 18 and linearization, one obtains two linear PDEs for the evolution of the amplitude modulation and phase modulation. Since the coefficients of these equations are independent of ξ and τ, a normal mode analysis reveals that non trivial solutions of the form $\delta = \Delta \exp\left[i\left(K\xi - \gamma\tau\right)\right]$ exist provided

$$\gamma^2 = K^2 L\left(2Ma_0^2 + K^2 L\right) \tag{19}$$

and the stability condition of the uniform wave train can be formulated for any given wavenumber *K*. When $LM < 0$, one can see that the uniform wavetrain is always unstable to perturbations with very long wavelength. This therefore corresponds to the condition of instability, whereas $LM > 0$ corresponds to stability.

When $LM < 0$, there exists a finite range of wavenumbers K over which the growth rate γ has a non zero imaginary part. To illustrate this we have plotted in figure 1 the imaginary part of γ or the growth rate of the modulation normalized by the maximum growth rate in the absence of vorticity as a function of the modulation wavenumber *K* normalized by $2a_0 k_0^2$. The curves in figure 1, which have been computed for a wave train of steepness $a_0 k_0 = 0.10$ and nondimensional depth $k_0 h = 2$, show that small positive velocity shear tends to enhance the sideband instabilities, whereas small negative velocity shear tends to suppress

instability. We use here a dimensionless vorticity defined as $\bar{\Omega} = \Omega_0 / \omega$.

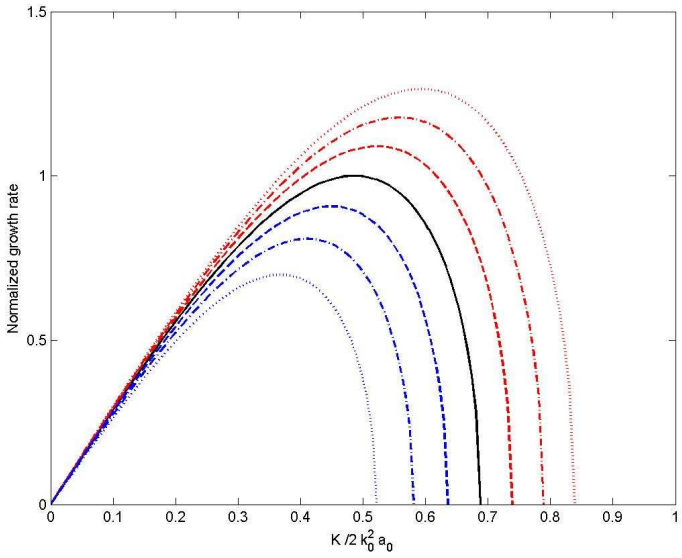

Figure 1. Normalized growth rate as a function of the perturbation wavenumber for $k_0 h = 2$ and $\bar{\Omega} = 0$ (solid line), $|\bar{\Omega}| = 0.1$ (dashed line), $|\bar{\Omega}| = 0.2$ (dot-dashed line), $|\bar{\Omega}| = 0.3$ (dotted line). Blues lines and red lines are associated with negative and positive velocity shear, respectively.

3. Numerical results

For numerical purposes, it is often more convenient to work with the governing equations in dimensionless form. By choosing deep water scalings, the governing equations (13) and (14) become

$$\partial_t \zeta = \left(1+\left(\partial_x \zeta\right)^2\right) W - \partial_x \zeta \cdot \partial_x \phi_s - \left(U + \Omega\zeta\right) \cdot \partial_x \zeta \tag{20}$$

$$\partial_t \phi_s = -\zeta - 0.5\left(\partial_x \zeta\right)^2 + 0.5\left[1+\left(\partial_x \zeta\right)^2\right] W^2 - \left(\delta + \Omega\zeta\right) \cdot \partial_x \phi_s + \Omega \psi_s \tag{21}$$

where $\delta = U_0 \sqrt{k_r / g}$ and $\Omega = \Omega_0 / \sqrt{g k_r}$ are dimensionless parameters, and k_r is the inverse of a reference length scale l_r. For a numerical domain containing n wavelengths of the carrier wave, the length of the domain is $L_x = n\lambda_0$. By choosing the reference length scale as $l_r = L_x / (2\pi)$, the dimensionless length of the numerical domain becomes $k_r L_x = 2\pi$ and the dimensionless spectral resolution $dk / k_r = 1$.

3.1. *Generation of nonlinear wave*

Given that we have no computer code to compute exact nonlinear travelling waves on a linear shear current and water of finite depth, we have decided to use an adjustment procedure that projects a linear wave onto a nonlinear progressive wave. In essence, we separate the linear parts of the right hand side of Eqs. 13-14, and the non linear terms are multiplied by the quantity

$$R = 1 - \exp\left[-\left(t / T_a\right)^{n_a}\right] \tag{22}$$

with $n_a = 4$ (rate of adjustment) and $T_a = 10 T_0$ (duration of the period of adjustment). Then these modified boundary conditions are integrated with a classical RK4 scheme and a constant time step.

As shown by Dommermuth (2000) for deep water waves and no background vorticity, this adjustment procedure allows linear solutions to be used as input to nonlinear free-surface simulations. The nonlinear interactions including bound and free harmonics can be generated to any order of approximation during the period of adjustment. Further, the numerical errors can be made arbitrarily small by either decreasing the rate of adjustment or increasing the duration of the period of adjustment.

In this subsection, we present numerical results for the case of finite depth and constant vorticity. In all cases presented below, the following initial conditions are prescribed:

$$\zeta = a_0 \sin\left(k_0 x\right) \qquad \phi_s = \frac{c_* a_0}{\tanh\left(k_0 h\right)} \sin\left(k_0 x\right) \tag{23}$$

where a_0 is the initial wave amplitude, k_0 the wave number and c_* the linear wave speed infinite depth without or with constant vorticity. In the former case $c_* = c_d = \sqrt{g \tanh\left(k_0 h\right)/k_0}$, while in the later case $c_* = \omega / k_0$ where ω is given in dimensionless form by the following equation:

$$\omega_* = \frac{\omega}{\sqrt{g k_0 \tanh\left(k_0 h\right)}} = \sqrt{1 + \left(\frac{\sigma \Omega_*}{2}\right)^2} - \frac{\sigma \Omega_*}{2} \tag{24}$$

where $\Omega_* = \Omega_0 / \sqrt{g k_0 \tanh\left(k_0 h\right)}$ is the dimensionless vorticity and $k_0 h$ represents the dimensionless undisturbed depth.

To demonstrate the validity of the adjustment procedure, we have considered $k_0 h = 2$ and an initial wave steepness $a_0 k_0 = 0.10$. In the case without vorticity, we have reference exact solutions that have been computed using the method of Longuet-Higgins (1987) and, therefore can validate accurately the adjustment procedure. In the presence of constant vorticity, however, we do not have exact reference numerical solutions at our disposal. We merely have approximations which are accurate up to the second-order, as described by Thomas (2012). Therefore, we will use these asymptotic results to validate the adjustment procedure.

Firstly, we validate the adjustment procedure in the case of finite depth without vorticity. To do this properly, we should take care in defining the steepness of initial linear wave, since we expect that the final steepness of the nonlinear wave, say ε will differ from the initial one $\varepsilon_0 = a_0 k_0$, as shown by Dommermuth (2000) in deep water. When this is done properly, we obtained the results plotted in figure 2 with 16 alias-free Fourier modes and two higher-order spectral approximations for the vertical velocity, namely *M = 6* and *M = 8*. The modal amplitudes of the first 16 harmonics are plotted as a function of dimensionless time. With *M = 6* one can see that only the 2nd through the 9th harmonics approach the exact Stokes solutions when *t* approaches the period of adjustment $T_a = 10 T_0$. By increasing the order of truncature in the HOS simulations, the matching is improved up to the 14th harmonics.

To illustrate the adjustment procedure in presence of vorticity, we have considered $k_0 h = 2$, an initial wave steepness $a_0 k_0 = 0.10$, and both negative ($\bar{\Omega} = -0.2$) and positive ($\bar{\Omega} = 0.2$) velocity shear. As in the first stage of validation, the HOS simulations are done with $n_a = 4$ and $T_a = 10 T_0$ for each value of the dimensionless vorticity $\bar{\Omega}$.

Figure 3 shows the results for the first eight modal amplitudes, as obtained from two higher-order spectral simulations, namely with *M = 3* and *M = 6*. It is seen that the adjustment scheme provides a gradual transition from linear initial conditions to an *M*th-order spectral approximation. Whatever the sign of $\bar{\Omega}$ and the values of M considered here, we can see that the modal amplitude of the 2nd harmonic approach the value predicted by the 2nd-order asymptotic theory. For the positive values of $\bar{\Omega}$ considered here, we can see that the modal amplitudes of the 2nd through the 4th harmonics approach values that are independent of *M*, when *t* approaches the period of adjustment T_a. However, for the negative values of $\bar{\Omega}$,

it appears that the spectral solutions differ depending on *M = 3* or *M = 6*, although the spectral amplitudes reach a steady regime beyond the period of adjustment. Taking *M = 8* improves slightly the results obtained with the HOS model, and further increasing *M* regularizes the spectrum over a broader range of harmonics (not shown).

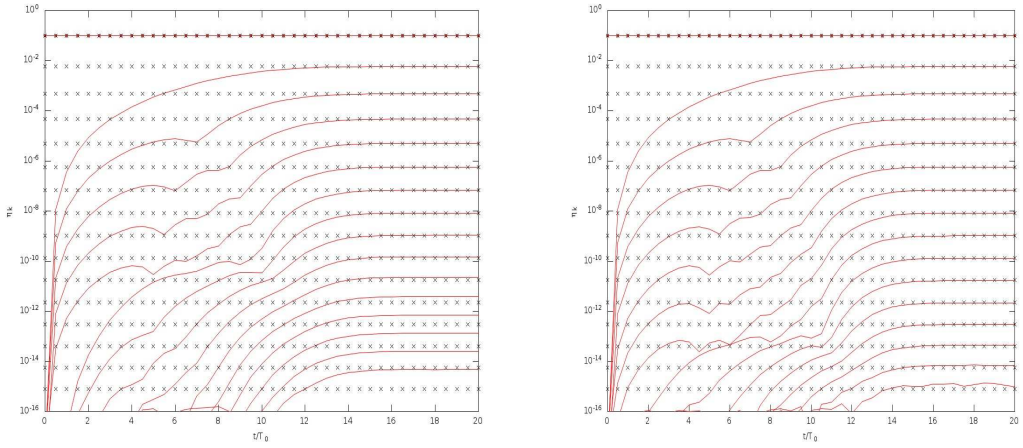

Figure 2. Adjusted Stokes wave simulation with $ak_0 = 0.10$, $\bar{\Omega} = 0$ and using 16 alias-free Fourier modes; (Left) with *M = 6*; (Right) using *M = 8*. The solid lines indicate the nonlinear HOS solution and the horizontal lines of crosses indicate the exact nonlinear progressive wave.

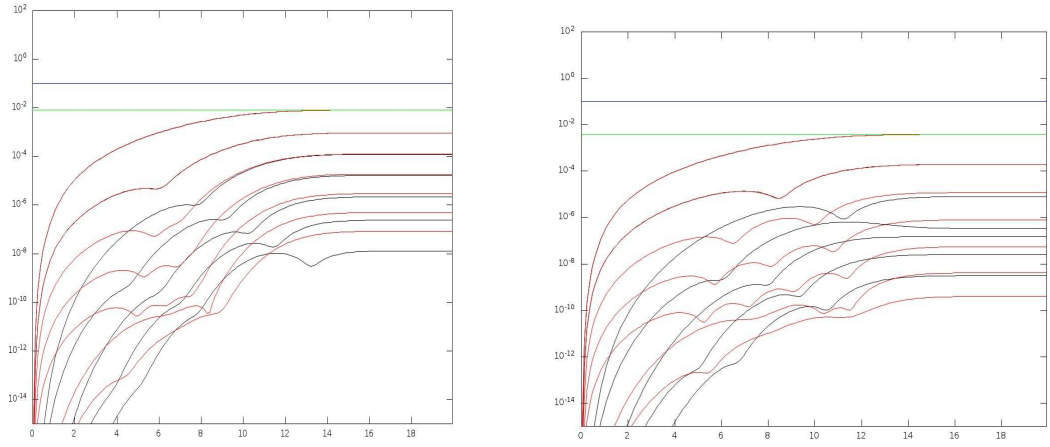

Figure 3. Adjusted Stokes wave simulation with $ak_0 = 0.10$, $\bar{\Omega} = 0.2$ (Left) and $\bar{\Omega} = -0.2$ (Right). The black curves refers to the simulations with *M = 3* and the red curves with *M = 6*. The horizontal green line represents the amplitude of the 2nd harmonic as predicted by the 2nd-order asymptotic theory.

3.2. *Benjamin Feir instability*

As already mentioned, the nonlinear evolution of the Benjamin-Feir or modulational instability of uniform wave trains in finite depth on a linear shear current has not been extensively studied. As described in the introduction, various theories based on multiple scales analysis are available for calculating the linear stability properties of weakly nonlinear uniform wave trains to long modulational perturbations, even for an arbitrary vorticity distribution. Considering a background linear shear current, Thomas et al. (2012) amongst others demonstrated that vorticity modifies significantly the modulational instability properties of weakly nonlinear uniform wave trains, namely the growth rate and bandwidth of the unstable side-band

modes.

Common to these theories is that they provide a basis to study only the early stages of wave-wave interactions due to the Benjamin-Feir instability and, therefore, little progress has been made beyond the weakly nonlinear regime. Only recently, within the framework of the fully nonlinear water wave equations, Choi (2009) considered the Benjamin-Feir instability of a modulated wave train in deep water with both positive and negative linear shear currents.

In this section we present numerical results obtained in a finite depth case and a linear shear current. The numerical simulations were performed using the vor-HOS formulation with a truncation order $M=3$, a non dimensional undisturbed depth $k_0h=2$ and different values of the vorticity of the background flow with $U_0=0$.

The initial condition consists of three Airy waves, two sidebands and one primary carrier wave of steepness $\varepsilon = a_0 k_0$ and wavenumber k_0. More specifically, we assume that

$$\zeta = a_0 \cos(k_0 x) + b\left[\cos\left((k_0 + \Delta k)x + \theta\right) + \cos\left((k_0 - \Delta k)x + \theta\right)\right] \tag{25}$$

Here the sidebands have wavenumbers slightly detuned from the carrier wavenumber, i.e. $k_\pm = k_0 \pm \Delta k$ where Δk represents the wavenumber of the amplitude modulation. Here θ represents the phase of the modulation. In this work the initial amplitudes of the sidebands are set to 10% of the carrier wave amplitude, i.e. $b=a_0/10$, and we choose $\theta = -\pi/4$ in all cases.

For a steepness $\varepsilon = 0.10$ the parameters k_0 and $\Delta k = pk_0$ are chosen in a such a way that the corresponding modulation corresponds to the most unstable sidebands when the background vorticity equals 0. For the given undisturbed depth and uniform wave train, this requirement is met by choosing $k_0=10$ and $p=1/10$. Hence the computational domain contains 1 modulation (10 carrier wavelengths). In all simulations the time integration were carried out for a duration of 500 carrier wave periods using a RK4 scheme with a constant time step size $dt=T_0/50$, where T_0 is the carrier wave period. Besides we set a cutoff wavenumber $k_m=5k_0$, implying that each carrier wave contains 20 numerical mesh points.

Figure 4 shows the results obtained first in the absence of background vorticity, namely with $\Omega = 0$. The results are shown for the carrier wave, the lower side-band and the upper sideband. The modulation-demodulation behaviour of the solution is clearly observed. As expected, the onset of the Benjamin-Feir instability is delayed by the adjustement scheme, but otherwise, there is no apparent effect on the growth rate of the Benjamin-Feir instability. As in the deep water case, we observe asymmetrical growth of the sidebands. The HOS solution predicts that the lower sideband grows faster than the upper sideband, which is in qualitative agreement with the predictions obtained with modified Schrodinger equations or Zakharov's integral equation, as well as with experiments in wavetank by Lake et al. (1977) who first reported on this phenomenon.

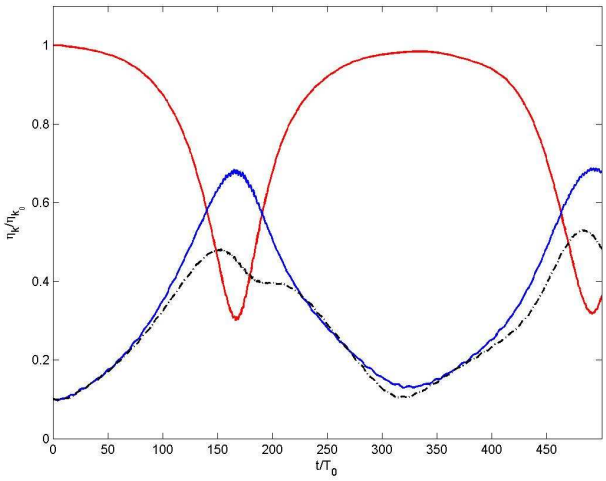

Figure 4. Normalized modal amplitudes of the carrier wave (red line), lower (blue line) and upper (black, dashed line) side-bands, for $\varepsilon = 0.10$, $kh = 2$ and $\bar{\Omega} = 0$.

Considering a small positive velocity shear, $\bar{\Omega} = 0.1$, tends to enhance the growth of the Benjamin-Feir instability, as shown in figure 5. By comparing with figure 4, one can also see that the strength of the interaction between the carrier wave and the sidebands is greater, as illustrated by the lower normalized amplitude of the carrier wave at the time of maximum modulation. Except for the growth rates of the lower and upper sidebands that are enhanced by a positive shear; their asymmetrical growth is not significantly modified during the first cycle of modulation-demodulation. The effect of the positive velocity shear is also seen in the recurrence period of the modulation-demodulation cycles, being lower for the case considered here as compared with the case without vorticity.

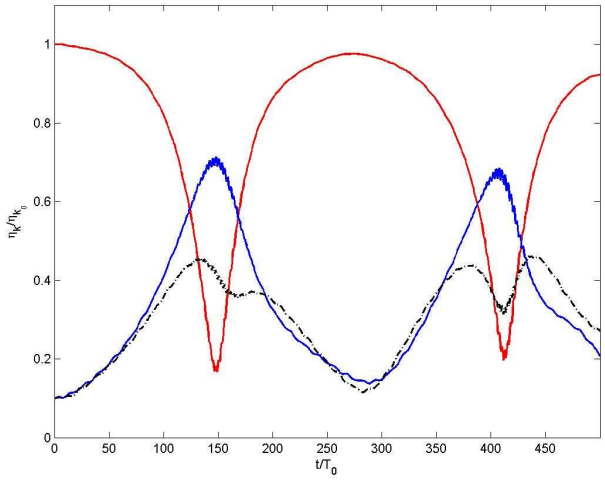

Figure 5. Normalized modal amplitudes of the carrier wave (red line), lower (blue line) and upper (black, dashed line) side-bands, for $\varepsilon = 0.10$, $kh = 2$ and $\bar{\Omega} = 0.1$.

In contrast the effect of a small negative velocity shear, $\bar{\Omega} = -0.1$, tends to reduce the growth of the Benjamin-Feir instability, as shown in figure 6. Not only the strength of interaction between the carrier wave and sidebands is reduced, but also the recurrence period of the modulation-demodulation cycle is increased significantly. Figure 6 also reveals that during the period of maximum modulation, the behaviour of the upper sideband differs from that observed in both previous cases.

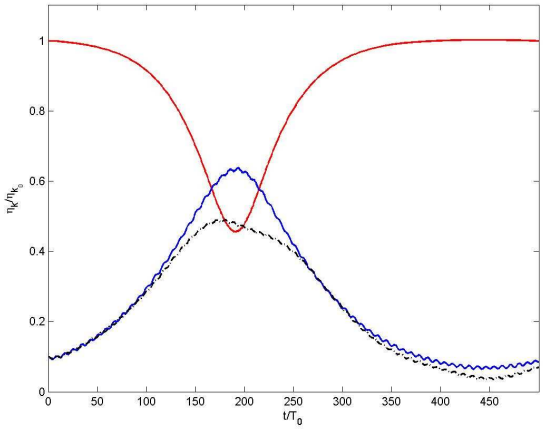

Figure 6. Normalized modal amplitudes of the carrier wave (red line), lower (blue line) and upper (black, dashed line) side-bands, for $\varepsilon = 0.10$, $kh = 2$ and $\bar{\Omega} = -0.1$.

For each case considered in this study, we show in figure 7 the time history of the ratio R of maximum amplification defined as $R=\zeta_{max}/a_0$. Here ζ_{max} represents the maximum amplitude of the envelope of wave crests that is observed during the development of modulational instability. We clearly see that a positive velocity shear enhance the growth rate of Benjamin-Feir instability and maximum modulation occurs sooner than in the case without vorticity. In contrast a negative velocity shear delays the onset of first maximum modulation.

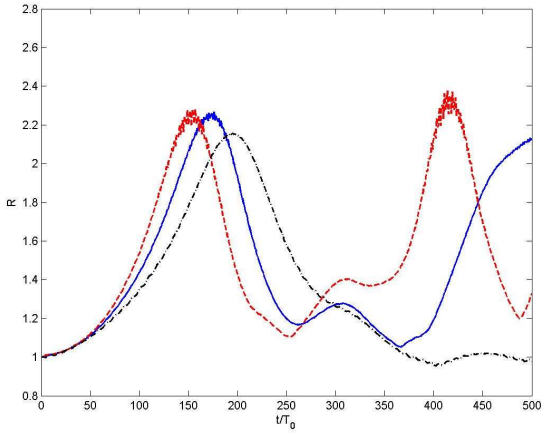

Figure 7. Time history of the ratio R of maximum amplification for $\bar{\Omega} = 0$ (solid line), $\bar{\Omega} = 0.1$ (red, dashed line) and $\bar{\Omega} = -0.1$ (black, dot-dashed line).

As reported by previous authors in the absence of vorticity, a short group of steep waves is formed at the maximum modulation. Similar observations hold here and we note that for the cases considered here the amplitude of the biggest waves, which occur at the time of maximum modulation, is little affected by the change of velocity shear. Knowing the results of Dold and peregrine (1999) for irrotational waves in deep water, which suggest that the maximum amplitude of these steep waves depends in a subtle manner on the phase relation between the amplitude modulation and the carrier wave, and given that $\theta = -\pi/4$ in all our simulations, it is not clear whether the steep wave events observed in our simulations correspond to the biggest modulation. It is also note trivial if the pair of side-bands that grows fastest also gives rise to the biggest modulation. In the future we will investigate these issues and, in particular, how changing the initial phase effects the growth of the modulation.

4. Conclusion

In this paper we have used an adaptation of the well-known high-order spectral method (HOS) to calculate the nonlinear time evolution of small amplitude modulations on two-dimensional wave trains in finite depth and in the presence of a linear shear current. An adjustment procedure for initializing the nonlinear free surface simulations with linear solutions has been validated both with and without constant vorticity. The nonlinear stability of a uniform wave train to sideband disturbances is modified by the effect of the linear shear current. In conclusion, we have shown that a small positive velocity shear tends to enhance the sideband instabilities, whereas small negative velocity shear tends to suppress instability. The HOS extension to linear shear current can be used to study the effect of larger velocity shear on the nonlinear stability of uniform wavetrains.

References

Bretherton, F.P. and Garrett, C.J., 1968. Wavetrains in inhomogeneous moving media. *Pr. R. S. Lond. A*, 302: 529-554.

Brevik, I., 1979. Higher-order waves propagating on constant vorticity currents in deep water. *Coast Eng*, 2: 237-259.

Choi, W., 2009. Nonlinear surface waves interacting with a linear shear current. *Math. Comput.Simulation*, 80: 101-110.

Constantin, A., 2011. Two-dimensionality of gravity water flows of constant non zero vorticity beneath a surface wave train. *Eur. J. Mech. B/Fluids*, 30: 12-16.

Dalrymple, R.A., 1974. A finite amplitude wave on a linear shear current. *J. Geophys. Res.*, 79: 4498-4504.

Dold, J.W. and Peregrine, D.H., 1986. Water-Wave Modulation. *Proc. 20th In. Conf. Coast Eng*, Taipei, Vol. 1: 163-175.

Dommermuth, D.G. and Yue, D.K.P., 1987. A high-order spectral method for the study of nonlinear gravity waves. *J. Fluid Mech.*, 184: 267-288.

Dommermuth, D., 2000. The initialization of nonlinear waves using an adjustment scheme. *Wave Motion*, 32: 307-317.

Johnson, R.S., 1976. On the modulation of water waves on shear flows. *Proc. R. Soc. Lond. A.*, 347: 537-546.

Jonsson, I.G., 1990. Wave-current interactions. *In The Sea*, pp: 65-120, J. Wiley and Sons.

Kishida, N. and Sobey, R.J., 1988. Stokes theory for waves on a linear shear current. *J. Engng Mech.*, 114: 1317-1334.

Ko, J. and Krauss, W., 2008. Effect of vorticity on steady water waves. *J. Fluid Mech.*, 608: 197-215.

Lake, B.M. and Yuen, H.C. and Rungaldier, H. and Ferguson, W.E., 1977. Nonlinear deep-water waves. Theory and experiment. Part 2, Evolution of a continuous wave train, *J. Fluid Mech.*, 83: 49-74.

Liu, Y. and Yue, D.K.P., 1998. On generalized Bragg scattering of surface waves by bottom ripples. *J. Fluid Mech.*, 356: 297-326.

Longuet-Higgins, M.S. and Stewart, R.W., 1961. The changes in amplitude of short gravity waves on steady non-uniform currents. *J. Fluid. Mech.*, 10: 529-549.

Longuet-Higgins, M. S., 1988. Lagrangian moments and mass transport in Stokes waves. Part 2. Water of finite depth. *J. Fluid Mech.*, 186: 321-336.

Nwogu, O.G., 2009. Interaction of finite-amplitude waves with vertically sheared current fields. *J. Fl. Mec*, 627 179-23.

Oikawa, M. and Chow, K. and Benney, D.J., 1987. The propagation of nonlinear wave packets in a shear flow with a free surface. *Stud. Appl. Math.*, 76: 69-92.

Okamura, M. and Oikawa, M., 1989. The linear stability of finite amplitude surface waves on a linear shearing flow. *J. Phys. Soc. Japan*, 58: 2386-396.

Pak, O.S. and Chow, K.W., 2009. Free surface waves on shear currents with non-uniform vorticity: third order solutions. *Fluid Dyn. Res.*, 41:1-13.

Peregrine, D.H., 1976 Interaction of water waves and currents. *Adv. Appl. Mech.*, 16: 9-17.

Simmen, J.A. and Saffman, P.G., 1985. Steady deep-water waves on a linear shear current. *Stud. Appl. Math.*, 75: 35-57.

Smith, R.A., 1998. An operator expansion formalism for nonlinear surface waves over variable depth. *J. Fluid. Mech.*, 363: 333-347.

Teles Da Silva, A.F. and Peregrine, D.H., 1988. Steep surface waves on water of finite depth with constant vorticity. *J. Fluid Mech.*, 195: 281-02.

Thomas, G.P. and Klopman, G., 1997. Wave-current interactions in the near shore region. In Gravity waves in water of finite depth. *J.N. Hunt: Advances in Fluid Mechanics*, 255-319, Computational Mechanics Publications.

Thomas, R., 2012. L'instabilité modulationnelle en présence de vent et d'un courant cisaille uniforme. *Thèse* Aix-Marseille.

Thomas, R. and Kharif, C. and Manna, M., 2012. A nonlinear Schrödinger equation for water waves on finite depth with constant vorticity. *Phys. Fluids 24*, 127102.

Tsao, S., 1959. Behaviour of surface waves on a linearly varying flow. *Tr. Mosk. Fiz.-Tekh. Inst. Issled. Mat.*, 3: 66-84.

West, B.J. and Brueckner, K.A. and Janda, R.S. and Milder, D.M. and Milton, R.L., 1987. A new numerical method for surface hydrodynamics. *J. Geophys. Res.*, 92: 11803-11824.

Whitham, G.B., 1965. A general approach to linear and nonlinear dispersive waves using a Lagrangian. *J. Fluid Mech.*, 22: 273-283.